

Combustion synthesis and preliminary luminescence studies of $\text{LiBaPO}_4 : \text{Tb}^{3+}$ phosphor

C B PALAN^{1,*}, N S BAJAJ¹, A SONI², M S KULKARNI² and S K OMANWAR¹

¹Department of Physics, Sant Gadge Baba Amravati University, Amravati 444602, India

²Radiological Physics and Advisory Division, Bhabha Atomic Research Centre, Mumbai 400094, India

MS received 28 April 2015; accepted 8 June 2015

Abstract. The polycrystalline sample of $\text{LiBaPO}_4 : \text{Tb}^{3+}$ (LBPT) was successfully synthesized by solution combustion synthesis and studied for its luminescence characteristics. The thermoluminescence (TL) glow curve of LBPT material consists of two peaks at 204.54 and 251.21°C. The optimum concentration was 0.005 mol to obtain the higher TL intensity compared to commercial TLD-100 phosphor. The peak shape method was used to calculate kinetic parameter (activation energy and frequency factor). In CW-OSL mode its sensitivity for beta exposure was found to be 50% compared to commercially available $\alpha\text{-Al}_2\text{O}_3 : \text{C}$ and 40% than LMP (BARC), and photoluminescence spectrum of LBPT shows green emission when excited with 225 nm UV source.

Keywords. Combustion synthesis; photoionization cross-sections; TL; OSL; PL.

1. Introduction

The use of combustion synthesis has been extensively spread and developed looking at experiences of last few years in the synthesis of luminescent materials, specifically borates, silicates, aluminates, and oxides.¹ The advantages of using the combustion method were low cost, highly effective as well as time saving approach to produce highly stable particles. Moreover, under some specific conditions, uniform, narrow distribution of particle with regular size crystallite could be obtained by the combustion method. Thus, the striking features of combustion synthesis make it attractive as well as focus on research for more development.

On the basis of the above consideration, it was decided to attempt the solution combustion method for the synthesis of LiBaPO_4 activated with Tb^{3+} ions. The LiBaPO_4 host provides a very good applicability in luminescence and other fields also.² Some attractive chemical and physical properties of LiBaPO_4 host make it prominent in the improvement of its ability in thermoluminescence (TL) application, when doped with rare earth (RE) ions.^{3–6} However, there are few reports found on the LiBaPO_4 phosphor and all are concentrated only on photoluminescence (PL) studies, while always activated with different RE ions.^{7,8} Thus, the prepared material was studied for TL, optically stimulated luminescence and PL properties. It was also noticed that the researchers who worked on the LiBaPO_4 phosphor mainly utilized sophisticated method of solid-state diffusion for synthesis.

In our previous paper, Tb-doped LiBaPO_4 phosphors synthesis by the combustion method and elementary results of TL and OSL properties of prepared phosphor were reported.⁹

In the present paper, $\text{LiBaPO}_4 : x\text{Tb}^{3+}$ ($x = 0.001, 0.002, 0.005, 0.01$ and 0.02) phosphor synthesis by using the combustion method was studied and phosphor characterizations were carried out by using X-ray diffraction (XRD), scanning electron microscopy (SEM) and luminescence properties (TL, OSL and PL) of this prepared phosphor. Also the concentration quenching of Tb activators was calculated and kinetics parameter of TL glow curve of $\text{LiBaPO}_4 : \text{Tb}^{3+}$ phosphor was determined.

2. Experimental

As discussed, researcher worked on LiBaPO_4 phosphor always used solid-state reaction for synthesis.¹⁰ However, there were no reports on the use of combustion synthesis for such compound. The emphasis on combustion synthesis was only due to drawbacks of solid-state diffusion.^{11,12}

During the reaction, all AR grade constituent raw materials were used such as lithium nitrate (LiNO_3), barium nitrate (BaNO_3)₂, ammonium dihydrogen orthophosphate ($\text{NH}_4\text{H}_2\text{PO}_4$), ammonium nitrate (NH_4NO_3) and urea ($\text{NH}_2\text{-CO-NH}_2$). While synthesis, the precursors were mixed thoroughly in China clay basins. The stock solution of the dopant Tb_4O_7 was then added into the mixture and later little amount of double distilled water was added into the prepared mixture. The mixture slowly converts into the thick paste. The thick paste was then heated for 5–10 min on hot plate, till it turns into a homogeneous clear solution. The clear solution obtained was then transferred directly to preheated furnaces maintained at temperature of 550°C. The clear solution was warmed and boiled till the evolution of lots of fumes, for 5 min. As the fuel reaches the required temperature for

* Author for correspondence (chetanpalan27@yahoo.in)

Table 1. Molar ratio and weights of the ingredients for $\text{LiBaPO}_4 : \text{Tb}^{3+}$.

Product	Corresponding reaction with balance molar ratios of precursors
$\text{LiBa}_{(1-x)}\text{PO}_4 : x \text{Tb}^{3+}$	$\text{Li}(\text{NO}_3) + \text{NH}_4\text{H}_2\text{PO}_4 + \text{Ba}(1-x)(\text{NO}_3)_2 + 5\text{CO}(\text{NH}_2)_2 + 7.5\text{NH}_4\text{NO}_3 + x(\text{Tb}_4\text{O}_7 + \text{HNO}_3) \rightarrow \text{LiBa}_{(1-x)}\text{PO}_4 : x \text{Tb}^{3+} + \text{gaseous products}$

burning, the self-heat generating redox reaction was started. The presence of the oxidizer in the reaction, i.e., ammonium nitrate increases the enthalpy of reaction and so the reaction time. The temperature of environment during the reaction may be around 1100–1200°C. This sudden high temperature generation from the fuel and oxidizer reaction increases the chances of the formation of fine and stable product. The fine powder of $\text{LiBaPO}_4 : \text{Tb}^{3+}$ (LBPT) was then finally obtained. The powder obtained from the reaction was then sintered in the microwave furnace at 950°C for 2 h and directly quenched to room temperature. The step was introduced to remove excess of organic impurities and carbon traces remaining in the material after reaction. Also the sintering gives the particles with fine structure due to sudden quenching. The same process was repeated for the different concentration of dopant. The proposed chemical composition and molar ratio of the ingredients used are shown in table 1.

3. Characterization

The finally sintered samples were then subjected to various characterizations such as X-ray diffraction (XRD) and scanning electron microscopy (SEM) for structural and morphological conformation. The XRD used for analysis by using Rigaku miniflex X-ray diffractometer was with scan speed of 6.000 deg min^{-1} and with $\text{Cu K}\alpha$ radiation. The SEM result was obtained from Hitachi S-4800. For OSL/TL response, all the samples were irradiated using $^{90}\text{Sr}/^{90}\text{Y}$ beta source with the dose rate of 20 mGy min^{-1} . The CW-OSL studies were carried out using RISO TL/OSL system at Bhabha Atomic Research Center, Mumbai. The PL studies with constant 1 nm slit width for excitation and emission windows were carried out on Hitachi F-7000 fluorescence spectrometer equipped with a 450 W xenon lamp.

4. Results and discussion

4.1 Conformation of material

Figure 1 represents the XRD patterns of pure LiBaPO_4 and doped $\text{LiBaPO}_4 : x \text{Tb}^{3+}$ ($x = 0.001, 0.002, 0.005, 0.01$ and 0.02). The patterns were compared with the ICDD file (00-014-0270). They were in good agreement with the ICDD file in terms of peak position as well as intensity. However, there were no peaks found from dopant which support the complete dissolution of dopant at the proper lattice site in the host. Moreover, the identical nature of patterns confirms that the method could be implied for the synthesis of LiBaPO_4 .

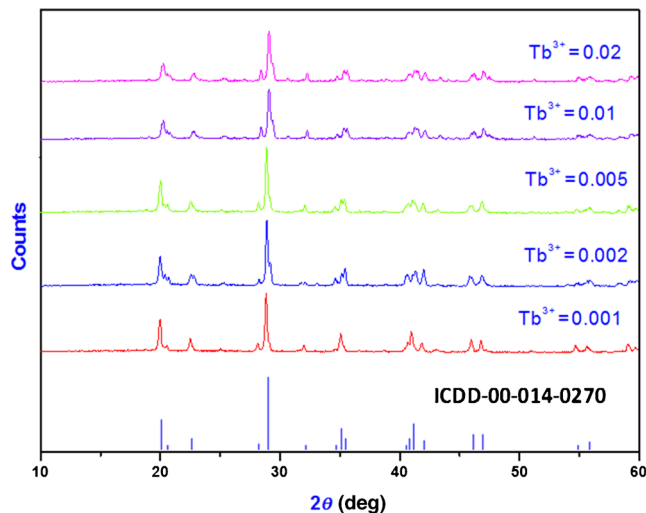


Figure 1. XRD pattern of pure and Tb^{3+} -doped LiBaPO_4 with standard ICDD file.

The XRD data can be refined to be hexagonal structure and crystallized in the P6_3 space group. However, in LiBaPO_4 lattice, the ionic radius of Tb^{3+} (1.095 nm, C.N. = 9) was closed to Ba^{2+} (1.47 nm, C.N. = 6) than the Li^+ (0.76 nm, C.N. = 9). Based on the effective ionic radii it was assumed that the Ba^{2+} was more preferably replaced by Tb^{3+} . However, due to the difference in the ionic radius was reflected by high angle shifting in main peak at 28.5° in pure LiBaPO_4 . The shifting was increased with the increase in concentration of Tb^{3+} , i.e., for 0.02 mol of Tb^{3+} , the main peak at 28.5° was shifted to 29.5°. ¹³

4.2 Morphological studies

SEM image (representative) is represented in figure 2 for the combustion synthesized LBPT phosphor. It indicates that in combustion synthesized phosphor, the particles are quite agglomerated but show regular stick-shaped morphology. The edges of crystallites are sharp and fine in structure; this may be observed due to indirect microwave sintering of sample at 950°C and sudden quenching. From the SEM image it was also confirmed that the particles are in submicron range.

4.3 TL behaviour

The TL of samples was recorded on exposure of sample packed in aluminium foil under 100 mGy beta-ray radiations. Figure 3 represents the TL glow curves for LiBaPO_4 doped with different concentrations of RE ion Tb^{3+} . The



Figure 2. SEM pattern for combustion synthesized $\text{LiBaPO}_4:\text{Tb}^{3+}$ phosphor.

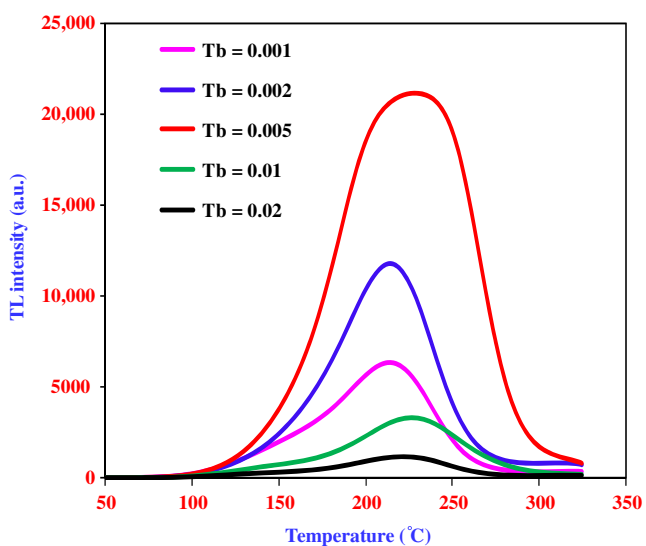


Figure 3. TL glow peaks for $\text{LiBaPO}_4:\text{Tb}^{3+}$ with different concentration.

TL glow curve consists of peak at temperature in the range 100–300°C. However, as the Tb^{3+} concentration increased the TL glow curve shifted towards higher temperature side at around 235.15°C. This temperature shifting to near about 5°C occurred may be due to multilevel or a continuous distribution of trap depth.¹⁴

At the same time, it was apparent that the intensity of the TL peak increases with the increase in the concentration of Tb^{3+} from 0.001 to 0.005 mol and then TL intensity decreases with the further increase in the concentration of the Tb^{3+} from 0.01 to 0.02 mol. The possible reason for quenching may be due to decrease in the quantum efficiency. Because when the content of Tb^{3+} ions was too high,

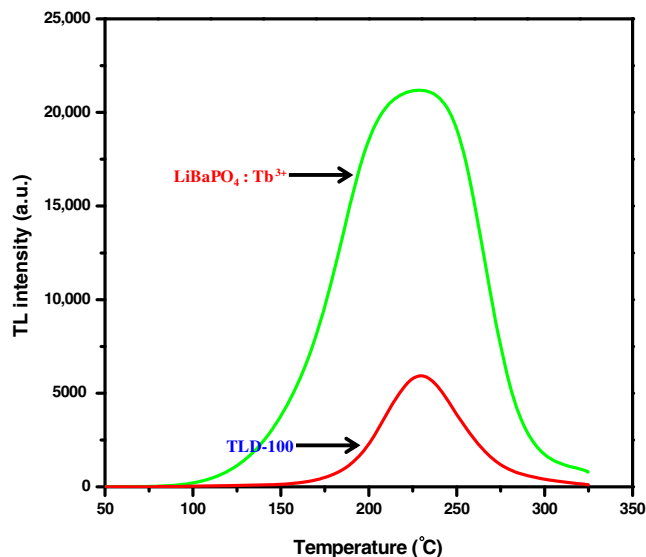


Figure 4. TL glow curve for $\text{LiBaPO}_4:\text{Tb}^{3+}$ compared with commercial phosphor TLD-100.

the energy transfer exceeds the energy emission. However, for 0.005 mol of Tb^{3+} the sample shows a broad peak and nonsymmetric peak with highest intensity.

4.4 Comparison of sensitivity with commercial TLD-100

The TL glow curve of LBPT for optimum concentration of Tb^{3+} (0.005 mol%) was compared with glow curve obtained from commercial TLD-100 for the same dose of exposure (i.e., 100 mGy). The comparative glow curves are represented in figure 4. It was clearly observed that LBPT exhibits nearly four times higher sensitivity than commercial TLD-100. Also, the material exhibits the peak in lower temperature but in dosimetric range than that of the TLD-100. The only drawback was Z -effective, the material required for personal dosimetry needs Z -effective compared to human tissue ($Z_{\text{eff}} = 7.4$). The Z -effective for LiBaPO_4 material was much higher than required and hence not applicable in personal monitoring. However, the material was quite useful in environmental as well as high-dose dosimetry but still need some confirmations on the laboratory scale that limits the applications.

4.5 Deconvolution and kinetic studies

Figure 5 shows deconvoluted curve for LBPT phosphor. By using peak fit software TL glow curve were deconvoluted for more resolved view of peaks inside the observed peak. From deconvoluted curve it was observed that the broad single peak consists of two symmetric peaks P_1 and P_2 at 204.54 and 251.21°C, respectively.

For the calculation of kinetic parameter such as activation energy and frequency factor of the glow peak, the easiest and most popular peak shape method was utilized.^{15–18} The activation energy for peaks P_1 and P_2 were found to be 1.28 and

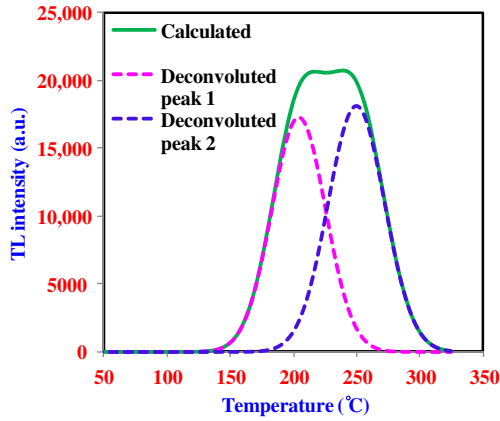


Figure 5. Deconvoluted curves from experimental curve for $\text{LiBaPO}_4:\text{Tb}^{3+}$.

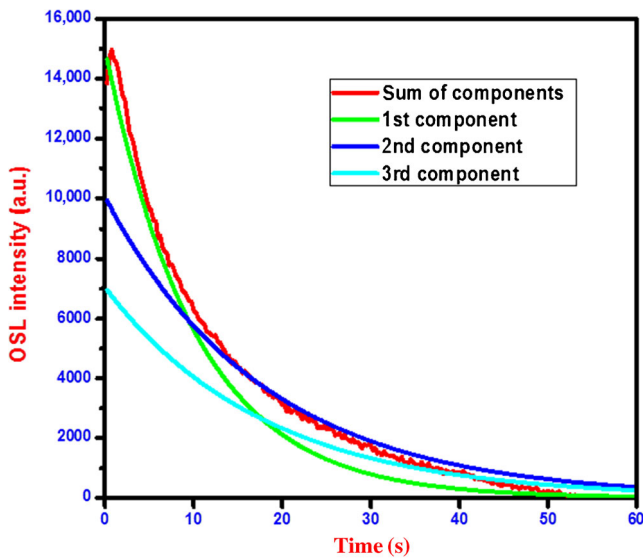


Figure 6. CW-OSL response of $\text{LiBaPO}_4:\text{Tb}^{3+}$ for 20 mGy beta dose. The third-order exponential fit on the decay curve shows the presence of three components.

1.553 eV, while frequency factor were found to be 1.02×10^{13} and $2.16 \times 10^{14} \text{ s}^{-1}$, respectively. Geometrical factor μg calculated for peaks P₁ and P₂ confirms second order of kinetic nature of the curve.

4.6 Optically stimulated luminescence

The sample was studied for its OSL response using blue LED stimulation (470 nm). Figure 6 shows the typical CW-OSL response of LBPT for 20 mGy beta dose. The third-order exponential fit on the decay curve shows the presence of three components. The best correlation is obtained for third-order exponential decay functions $y = A_1 \exp(-x/t_1) + A_2 \exp(-x/t_2) + A_3 \exp(-x/t_3) + y_0$. From fitting calculated value of $R^2 = 0.99812$ and $\chi^2 = 25543.03947$. For these three components the photo-ionization cross-sections were calculated and given in table 2. Figure 7 represents the

Table 2. Photoionization cross-sections of $\text{LiBaPO}_4:\text{Tb}^{3+}$.

Phosphors	Component	Photoionization cross-sections (cm^2)
$\text{LiBaPO}_4:\text{Tb}^{3+}$	First	9.03×10^{-17}
	Second	15.93×10^{-17}
	Third	15.93×10^{-17}

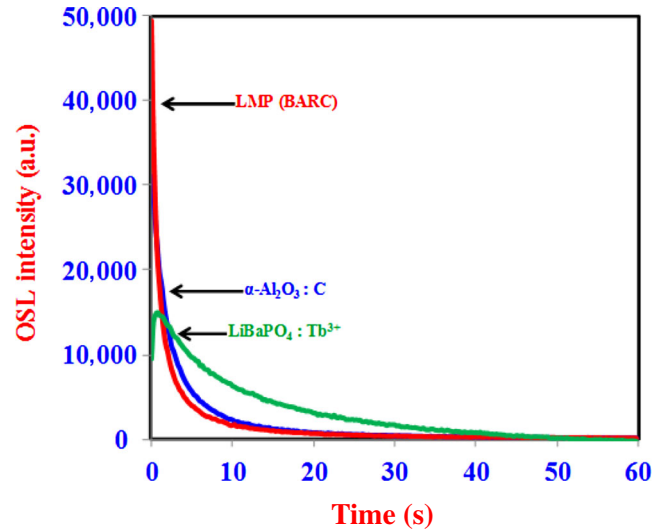


Figure 7. CW-OSL response of $\text{LiBaPO}_4:\text{Tb}^{3+}$ compared with commercial $\alpha\text{-Al}_2\text{O}_3:\text{C}$ and LMP (developed by BARC) for 20 mGy beta dose.

comparison of OSL sensitivity for beta exposure and was found to be 50% compared to commercially available $\alpha\text{-Al}_2\text{O}_3:\text{C}$ and 40% than $\text{LiMgPO}_4:\text{Tb}^{3+},\text{B}$ (LMP) (developed by BARC).¹⁹

4.7 Photoluminescence properties

Generally Tb^{3+} ions are used as an activator in phosphor for getting green or blue emission due to transitions of $^5\text{D}_3 \rightarrow ^7\text{F}_J$ ($J = 6, 5, 4, 3$ and 2) level of Tb^{3+} ions in the host lattice. The combined excitation and emission spectra of LBPT phosphor are shown in figure 8. The excitation and emission spectra were observed under 544 and 225 nm, respectively. The excitation spectra consist of one narrow peak at 225 nm corresponding to the $4\text{f}^8-4\text{f}^75\text{d}$ transition of Tb^{3+} . On the other hand, the emission spectrum consists of a relatively weak peaks at 417 and 438 nm corresponding to the $^5\text{D}_3$ to $^7\text{F}_J$ ($J = 5$ and 4), while strong peaks were observed at 486, 544, 585 and 627 nm corresponding to the $^5\text{D}_4$ to $^7\text{F}_J$ ($J = 6, 5, 4$ and 3) transition within the 4f^8 configurations of Tb^{3+} .²⁰ Among the emission lines from the $^5\text{D}_4$ state the dominant emission was observed at 544 nm, corresponding to the $^5\text{D}_4$ to $^7\text{F}_5$ transition observed at 225 nm excitation. The $^5\text{D}_4$ to $^7\text{F}_5$ observed emission line was the strongest nearly in all host crystals, when the few

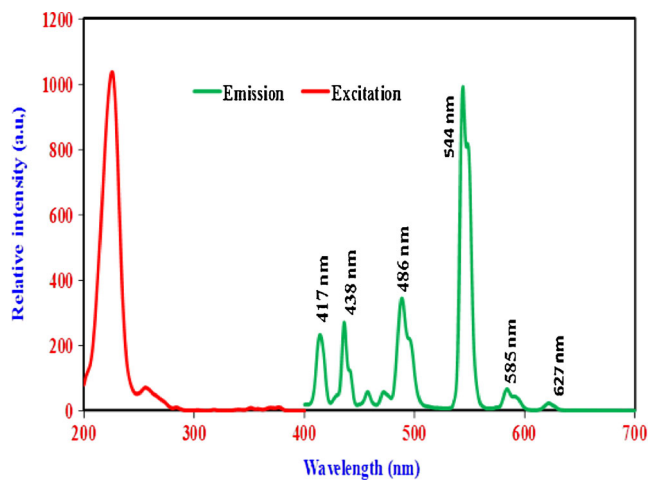


Figure 8. Excitation and emission spectra of $\text{LiBaPO}_4 : \text{Tb}^{3+}$.

or higher mole of Tb^{3+} concentration because this transition has the largest probability for both electric- and magnetic dipole-induced transitions.

5. Conclusions

Polycrystalline sample of LBPT was successfully prepared by solution combustion synthesis. The peak shape method was utilized to calculate the kinetic parameters, i.e., activation energy and frequency factor from the TL glow curve. In CW-OSL mode its sensitivity for beta exposure was found to be 50% compared to commercial available $\alpha\text{-Al}_2\text{O}_3 : \text{C}$ and 40% than LMP (developed by BARC). In TL mode sensitivity of this phosphor was found to be 4 times than that of TLD-100. This implies that LBPT phosphor may be useful in radiation dosimetry. Also the phosphor shows the characteristic strong green emission of Tb^{3+} ions when excited with 225 nm.

Acknowledgement

CBP is very much thankful to Head, Radiological Physics and Advisory Division, Bhabha Atomic Research Centre,

Mumbai 400 085, India, for providing the necessary facilities for the analysis of TL/OSL results.

References

1. Koparkar K A, Bajaj N S and Omanwar S K 2014 *Adv. Opt. Technol.* **5** ID 706459 5
2. Im W B, Yoo H S, Vaidyanathan S, Kwon K H, Park H J, Kim Y I and Jeon D Y 2009 *Mater. Chem. Phys.* **115** 161
3. Setlur A A, Radkov E V, Henderson C S, Her J H, Srivastava A M, Karkada N, Kishore M S, Kumar N P, Aesram D, Deshpande A, Kolodin B, Grigorov L S and Happek U 2010 *Chem. Mater.* **22** 4076
4. Happek U, Setlur A A and Shiang J J 2009 *J. Lumin.* **129** 1459
5. Srivastava A M, Comanzo H A, Camardello S S, Chaney B, Aycibin M and Happek U 2009 *J. Lumin.* **129** 919
6. Zhang X M, Li W L, Shi L, Qiao X B and Seo H J 2010 *Physica B: Lasers Opt.* **99** 279
7. Yang R Y and Lai H L 2014 *J. Lumin.* **145** 49
8. Zhang S, Nakai Y, Tsuboi T, Huang Y and Seo H J 2011 *Chem. Mater.* **23** 1216
9. Palan C B, Bajaj N S, Koul D K and Omanwar S K 2015 *Int. J. Lumin. Appl.* **5** 12
10. Wei D, Huang Y, Zhang S, Yu Y M and Seo H J 2012 *Appl. Phys. B* **108** 447
11. Bajaj N S and Omanwar S K 2013 *Opt. Mater.* **35** 1222
12. Koparkar K A, Bajaj N S and Omanwar S K 2015 *J. Rare Earth* **33** 486
13. Koparkar K A, Bajaj N S and Omanwar S K 2015 *Opt. Mater.* **39** 74
14. Upadhyay A K, Gulhare V, Dhoble S J and Kher R S 2011 *Indian J. Pure Appl. Phys.* **49** 382
15. Bajaj N S and Omanwar S K 2014 *J. Lumin.* **148** 169
16. Bajaj N S and Omanwar S K 2012 *J. Rare Earth* **30** 1005
17. Mckeever S W 1998 *Thermoluminescence of solids* (Cambridge: Cambridge University Press) p 88
18. Omanwar S K, Koparkar K A and Virk H S 2013 *Defect. Diffus. Forum* **347** 75
19. Dhabekar B, Menon S N, Alagu Raja E, Bakshi A K, Singh A K, Chougankar M P and Mayya Y S 2011 *Nucl. Instrum. Methods: Phys. Res. Sect. B* **269** 1844
20. Shaat S K K, Swart H C and Ntwaeaborwa O M 2014 *J. Alloys Compd.* **587** 600